# Energetic and Exergetic Performance Analyses of Solar Dish Based CO$_2$ Combined Cycle

## S. Mukhopadhyay[1], S. Ghosh[2*]

Department of Mechanical Engineering, Bengal Engineering and Science University,
Shibpur, Howrah 711 103, West Bengal, India
E-mail: [1]soumitra1995@gmail.com, [2]sudipghosh.becollege@gmail.com

### Abstract

This paper presents a conceptual configuration of a solar dish based combined cycle power plant with a topping gas turbine block and a bottoming steam turbine cycle coupled through a heat recovery steam generator (HRSG). Carbon dioxide has been considered as the working fluid for the topping cycle and it has been considered in gaseous state all through the cycle. Two-stage compression has been proposed for the carbon dioxide cycle. The conventional GT combustion chamber is replaced by a high-temperature directly irradiated annular pressurized receiver (DIAPR) consisting of cavity and tubular sections. Detail thermodynamic study has been performed for varying second stage pressure ratioand for varying gas turbine inlet temperature for the combined cycle keeping first stage pressure ratio fixed at 3.The gas turbine inlet temperature has been varied from 625$^O$ C to 900$^O$ C. The study reveals that work output of the combined cycle is maximum when the pressure ratio of the second stage compression is 2. Parametric exergetic analysis has also been performed for the components like dish, solar receiver and stack. The exergy analysis shows that the solar receiver contributes to maximum exergy destruction.

*Keywords: Solar dish; combined cycle; CO$_2$; thermal efficiency; exergy.*

## 1. Introduction

The demand for energy has increased manifold in recent years due to increase of world population and due to the expansion of global industries to meet the demand of mankind. The energy demand is mainly met by the fossil fuel energy sources. The conventional fossil fuel based energy to electricity conversion systems produce carbon dioxide, which in turn produces global warming. To keep global warming in a tolerable frame, the Scientific Council of the German Government for Global Environmental Change (WBGU) recommends, based on a scenario of the IPCC (Intergovernmental Panel for Climate Change), to reduce CO$_2$-emissions on a global level by 30 % until 2050 [1].The combustion of fossil energy carriers produce pollutants like sulphur dioxide and nitrogen oxide, which contribute to the formation of acid rain. An incomplete combustion causes the emission of carbon monoxide, unburned hydrocarbons and sooty particles, which pollute the atmosphere. The Kyoto Protocol, which is the first internationally agreed policy, also suggests thestabilization and the reduction of the greenhouse gases in the atmosphere.

So, the growing demand of energy and its increasingimpact on eco-system are emphasizing the scientists, engineers and policy makers to think for renewable energy sources. Out of various renewable energy options like wind, geothermal, ocean energy etc., solar energy is an important option since it is an inexhaustible and large source of energy.The power from the sun intercepted by the earth is approximately 1.8·10$^{11}$ MW [2] which is many thousands of times larger than the present consumption rate on the earth of all commercial energy sources. Thus, in principle, solar energy could supply all the present and future energy needs of the world on a continuous basis. So the strategic use of solar energy option can lead to a cleaner environment and can effectively deal with the energy crises problems.

One of the most cost efficient ways of generating electricity from solar radiation is through a solar thermal power plant (STPP) utilizing concentrated solar power (CSP), which converts solar heat into electricity. CSP with thermal energy storage can provide the same operational attributes as a fossilfueled thermal power plant, but subject to availability of the solar insolation as cited in [3]. Concentrated solar power may be of trough based, power tower or dish based for electricity production. A lot of work has been done on trough or power tower systems using Rankine or Brayton cycle but limited work has been reported on dish based similar systems, which has been attempted here.
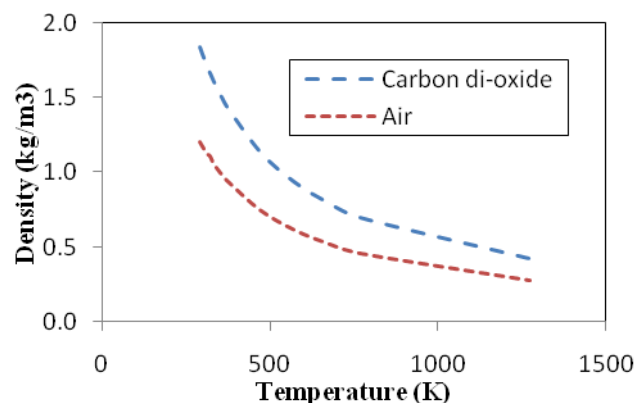


*Figure 1. Variation of density with temperature at atmospheric pressure.*

Like power tower and trough systems, a solar dish system can be tracked on two axes and a receiver is mounted at the focal point of the dish, where the working fluid is heated up by the concentrated solar power.
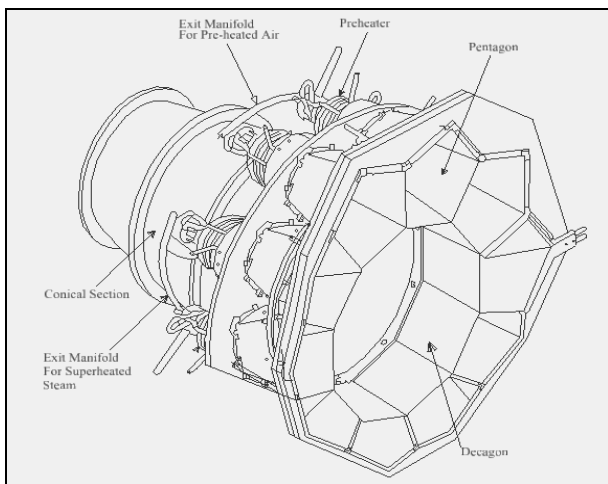


*Figure 2. Annular pressurized dual solar receiver [12].*

Large sizes of solar dishes are increasingly being considered in recent time. Development of solar concentrating dish of aperture area 500 m$^2$ at Australian National University has been reported and new designs for larger-size dishes have also been published [4]. It has also been suggested that larger size dishes are likely to be more cost-effective. These developments provided motivation for considering solar dishes in the present work.

Although a single dish system has been conceptualized in the present study, same simulation can effectively be applied to a double-dish or a multi-dish system depending on the technological development of solar dish.

The solar receiver considered in the present study is a directly irradiated annular pressurized receiver (DIAPR), which is a combination of cavity and tubular receiver sections. In case of cavity tubular receiver, less thermal and optical losses, reduced direct heat flux density on the absorber, a nearly uniform internal wall temperature, steady thermal performance and high solar absorption efficiency are achieved. It is also low cost and maintenance fee. The thermal losses of a solar cavity receiver include convection and radiation heat losses in the cavity and conduction heat loss through the insulation [5]. It has been suggested that such DIAPR can be applied to dish based system [6]. This type of receiver has several cavity and tubular sections. While cavity sections can be utilized for heating the gaseous working fluid ($CO_2$), the tubular sections can be shared for preheating gaseous working fluid and for producing superheated steam. Thus such receiver acts as a dual receiver. Use of dual receiver has also been reported by Buck et al. [7].

The carbon dioxide, which is otherwise discharged into the atmosphere as the by-product of combustion, can be utilized as the working fluid in the Brayton cycle since it is having various advantages. $CO_2$ exhibits excellent heat transfer properties and is non-flammable and non-toxic in nature [8]. It has relatively lower specific volume i.e. higher density in comparison to air, resulting in small size components for the same operating conditions. The variation of density for $CO_2$ and air at various temperatures

is shown in Figure 1, which has been done by using RefpropMini software and the figure shows that density of carbon dioxide is higher in comparison to air at various temperatures.

In the power generation system, exergy analysis or second law analysis has proven to be a powerful tool in thermodynamic analyses of the system. Exergy is defined as the maximum useful work that can be obtained when a system interacts with a reference environment, generally atmospheric conditions [9]. It also quantifies the process where exergy destruction is maximum i.e. exergy analysis provides a guideline for the process improvement.

The literature survey shows that very limited works are available for the energy and exergy analysis of solar dish based combined cycle power plant. In this regard, the present study proposes a conceptual configurationfor solar dish based combined cycle using carbon dioxide as the working fluid for the topping Brayton cycle and a simple downstream HRSG has been integrated with the topping cycle.A theoretical framework for the energy and exergy analyses of the solar dish based combined cyclehasbeen done for the proposed configuration and detail parametric analysis has been performed for the combined cycle from the energetic as well as exergetic point of view. The receiver considered in the present study is shown in Figure 2.

## 2. System Description of Proposed of Solar Dish Based Combined Cycle Power Plant

Figure 3 depicts the schematic of a solar dish based gas turbine combined cycle considered in the present study where carbon dioxide has been considered as the working fluid in the topping Brayton cycle. In the carbon dioxide based combined cycle, gaseous carbon dioxide at temperature 35$^O$C and pressure 25 bar enters the first stage compressor (COMP I) and a fixed pressure ratio of 3 has been considered for this stage to get the output pressure of carbon dioxide at 75 bar which is well above the critical pressure of carbon dioxide (73.8 bar). After compression in the first stage compressor, carbon dioxide is cooled in the intercooler to the initial temperature to reduce the volume of the gas. Then the carbon dioxide is compressed in the second stage compressor (COMP II) to a maximum pressure of 225 bar, which is possible to achieve as reported by Chacarteguiet et al. [10] depending on the pressure ratio.The compressed carbon dioxidethen enters into the solar receiver, mounted at the focal point of the solar dish. The receiver considered here is constructionally similar with the Directly Irradiated Annular Pressurized Receiver (DIAPR) as reported by Kribus et al. [11]. But the difference is that superheating of steam is also proposed in the same receiver, which is shown in Figure 2 and has been discussed later.

Since the maximum temperature achievable with this type of receiver is 1300$^O$C [6], the maximum gas turbine inlet temperature (TIT) considered here is 900$^O$C.The hot carbon dioxide now enters into the first gas turbine (GT I), which is solely dedicated to deliver power for both the compressors, COMP I and II. The exhaust from the GT I enter into the second gas turbine (GT II or power turbine) and it is coupled with a generator to get the power from topping Brayton cycle.
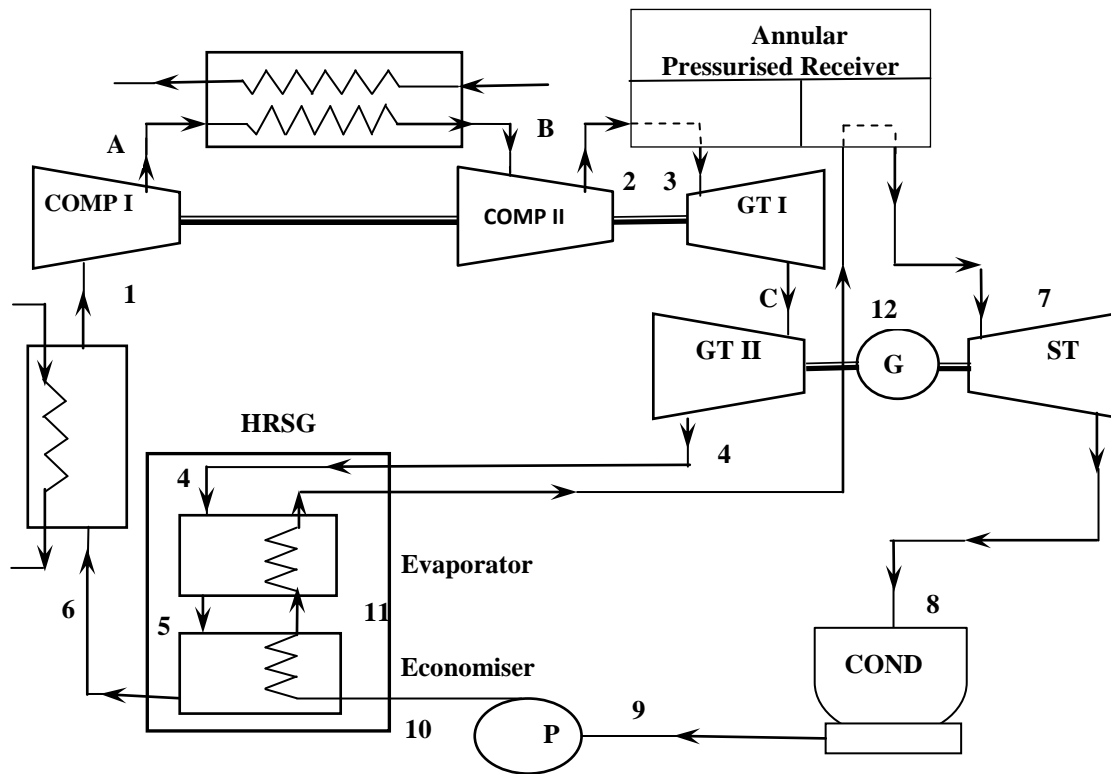
Figure 3.Carbon dioxide combined cycle power plant.

This exhaust from GT is passed through a heat recovery steam generator (HRSG) to produce saturated steam. In the HRSG, heat contained in carbon dioxide is first used to change the phase of the saturated water at 65 bar and 553.85 K (which is the saturation temperature of water at 65 bar) to saturated steam at Evaporator (EVAP) i.e. from state point 11 to state point 12 and finally, the heat energy remained in the exhaust $CO_2$ from the gas turbine is utilized to heat the feed water in the economiser (ECO) from point 10 to 11. Then the $CO_2$ returns to the COMP I through a heat-exchanger, releasing here necessary amount of heat to reach compressor inlet conditions. Saturated steam from evaporator i.e. from state point 12 is passed to the receiver againto convert it into superheated steam at 733K by the concentrated solar energy i.e. from state point 12 to point 7. The solar receiver considered here [11] can accommodate total ten numbers of cavity tubular receivers, out of which four numbers will be utilized for preheating the carbon dioxide and the remaining six numbers can be utilized for producing superheated steam required in the bottoming cycle [12].The superheated steam at point 7 (65 bar pressure and 733K) enters into the steamturbine (ST), and after producing work in the steam turbine, steam is exhausted in the condenser (COND) at point 8 at0.07 bar pressure. After being condensed in the condenser, water is pumped from point 9 to point 10 i.e. at the boiler pressure by a feed pump (P). The system as well as the coding in C language is developed in such a way that the temperature difference between the evaporator exit temperature of carbon dioxide and the saturation temperature of water (i.e. $T_{11}=T_{12}$) does not fall below $15^O$C for better heat transfer. The main assumptions for the carbon dioxide Brayton cycle are shown in Table 1.The p-h diagram of Brayton cycle with Carbon dioxide as the working fluid is shown in Figure 4.
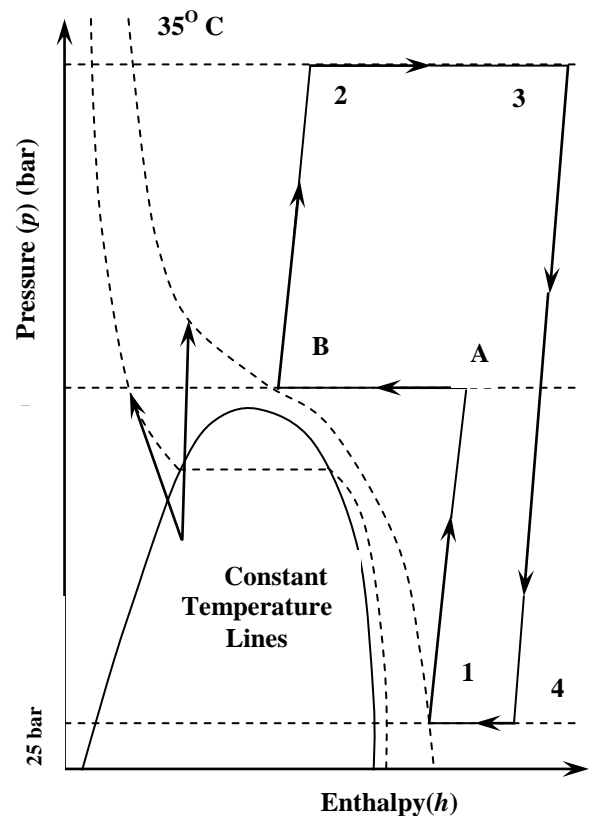


Figure 4. p-h diagram of Brayton cycle with Carbon dioxide.

Since this paper only considers the energetic and exergetic performance of the combined cycle at steady state, the thermal storage sub-systemhas not been discussed and notshown in Figure 3. The pressure drop in the solar receiver has been considered as 0.12 bar [13].

| Characteristics | Value |
|---|---|
| Maximum pressure ratio | 9 |
| Maximum TIT | $900^oC$ |
| Compressor inlet temperature | $35^oC$ |
| Compressor inlet pressure | 25 bar |
| Saturation pressure of water | 65 bar |
| Specific heat ratio of $CO_2$ | 1.3 |
| Superheat temperature | $460^oC$ |

## 2.1 Single-Shaft Two-Turbine Generator

In the present study, a single-shaft two-turbine configuration has been considered for the power block, where a GT and a ST together drive a generator. The first stage of the GT (GT I) solely drives the compressors and doesn't contribute to the power generation. The second stage of GT (GT II) and the ST have been placed on two ends of the generator, a configuration that has been in practice [14]. Each gas turbine is directly coupled to the generator and the steam turbine is connected through a clutch arrangement. The arrangement is shown in Figure 5.
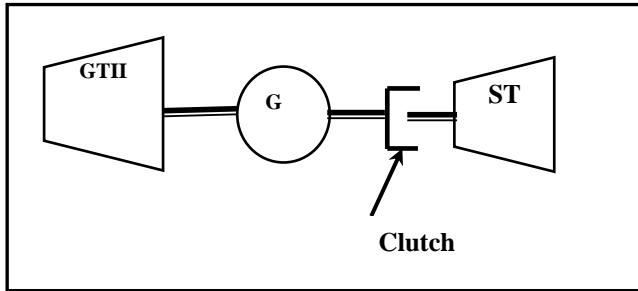


Figure 5. Single shaft two-turbine arrangement.

## 3. Methodology Adopted in the Present Study

The temperature–entropy diagram of the carbon dioxide based combined cycle plant is shown in Figure 6.The combined cycle has been analysed based on the following energy and exergy tools. The basic assumptions considered in the present study are as under:

a) Isentropic efficiency of compression=0.88
b) Unit mass flow rate (1 kg/s) of working fluid ($CO_2$) has been considered
c) Isentropic efficiency of expansion=0.90
d) Dish efficiency has been considered as 90% [15]
e) Receiver efficiency 82% [13]

## 3.1 First Law Analysis

The first law analysis or the energy analysis of the topping $CO_2$ Brayton cycle, bottoming HRSG and the combined cycle is done based on the following methodology.

### 3.1.1 Topping Brayton Cycle

The temperature of carbon dioxide at the end of first stage compression is given by the following equation

$$T_A = T_1 + \frac{1}{\eta_C}(T_{A'} - T_1) \tag{1}$$

Since perfect intercooling has been considered, $T_B = T_1$.

The temperature of carbon dioxide at the end of second stage compression is given by the following equation

$$T_2 = T_B + \frac{1}{\eta_C}(T_{2'} - T_B) \tag{2}$$
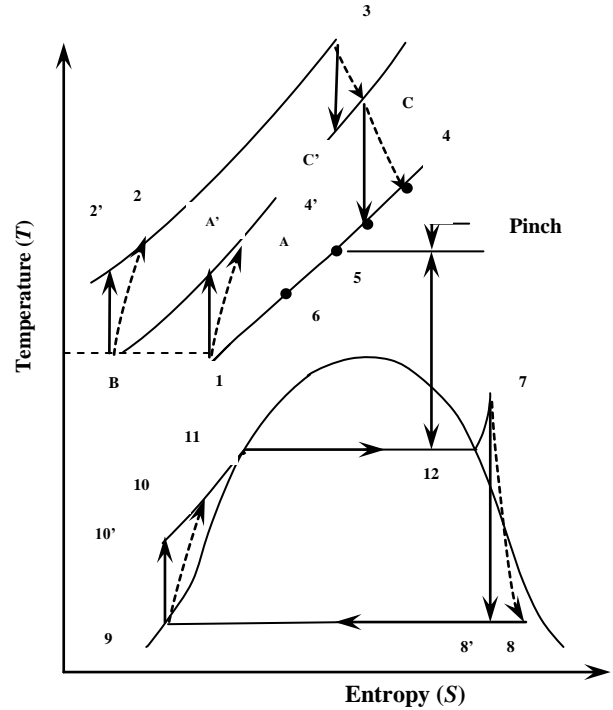


Figure 6. T-S diagram of carbon dioxide combined cycle plant.

Total compressor work is given by

$$W_{comp} = \left[ (h_A - h_1) + (h_2 - h_B) \right] \tag{3}$$

Required solar energy to reach the gas turbine inlet temperature can be obtained from the following equation

$$Q_1 = \frac{(h_3 - h_2)}{\eta_{dish}\eta_{receiver}} \tag{4}$$

**GT I** is dedicated for supplying the necessary power for both the compressors as per the following equation, neglecting the losses

$$(h_3 - h_C) = \left[ (h_A - h_1) + (h_2 - h_B) \right] \tag{5}$$

The temperature after first stage expansion $(T_C)$ is calculated by the method of interpolation.

The temperature at the end of second stage expansion is calculated from the following equation

$$T_4 = T_C - \eta_E (T_C - T_{4'}) \tag{6}$$

Net work obtained from the topping Brayton cycle or **GT II** is

$$W_{net,GT} = h_C - h_4 \tag{7}$$

### 3.1.2 Bottoming HRSG Plant

Initially, mass flow rate of steam in HRSG plant can be calculated from the overall energy balance equation in the HRSG:

$$m_w = \frac{(h_4 - h_6)}{(h_{12} - h_{10})} \quad (8)$$

Initially, $T_6$ is taken as $120^0$ C. Correct $T_6$ is found out later. $T_5$ can be found out from the energy balance in the evaporator:

$$mC_p(T_4 - T_5) = m_w(h_{12} - h_{11}) \quad (9)$$

Based on Eq. (8), first $m_w$ is calculated and subsequently from equation Eq. (9), $T_5$ is found out. $T_5$ Should be minimum $15^O$ C more than the saturation temperature of water. If the calculated $T_5$ does not satisfy this condition, $m_w$ is reduced by 0.0001 Kg/s and $T_5$ is recalculated. The process is repeated until $T_5$ satisfies the above condition and finally corrected $T_6$ is calculated from the following energy balance equation in economizer:

$$T_6 = \left[ T_5 - \frac{m_w(h_{11} - h_{10})}{mC_p} \right] \quad (10)$$

Heat energy required to raise the saturated steam to the required superheat condition is given by

$$Q_2 = \left[ \frac{m_w(h_7 - h_{12})}{\eta_{dish}\eta_{receiver}} \right] \quad (11)$$

Overall thermal efficiency is given by

$$\eta_{th,overall} = \left[ \frac{W_{net,GT} + W_{ST}}{(Q_1 + Q_2)} \right] \quad (12)$$

### 3.2 Exergy Analysis

The importance of second law based exergy analysis has already been discussed. Exergy is a generic term that defines the maximum possible work potential of a system from a stream of matter and or heat interaction with respect to the state of the environment being used as the datum state at 1.01325 bar and 298K [16]. In this sub-section, exergy analyses used for the different components will be discussed. Exergy balance of an irreversible system in steady state can be defined as:

$$Ex_{loss} = (Ex_{in} - Ex_{out}) \quad (13)$$

### 3.2.1 Solar Dish Sub-System

If $Ex_Q$ is the exergy corresponding to the solar radiation incident on the dish and the $Ex_{rec.}$ is the exergy delivered to the receiver, then the exergy balance for the dish sub-system is given by

$$Ex_Q = Ex_{rec} + Ex_{dest} \quad (14)$$

where,

$$Ex_Q = Q\left(1 - \frac{T_o}{T_{sun}}\right) \quad (15)$$

$$Ex_{rec} = Q_{rec}\left(1 - \frac{T_o}{T_{sun}}\right) \quad (16)$$

$$Q_{rec} = \eta_{dish}Q \quad (17)$$

Then the exergetic efficiency of the dish sub-system is given by the following equation:

$$\eta_{dish} = \frac{Ex_{rec}}{Ex_Q} \quad (18)$$

### 3.2.2 Solar Receiver Sub-System

The solar receiver considered here will be utilized to heat the compressed carbon dioxide as well to produce superheated steam. The exergy destroyed and the exergetic efficiency of the dish sub-system can be calculated from the Eqs. (19) and (20).

$$Ex_{dest,rec} = Ex_{rec} + (Ex_2 - Ex_3) + (Ex_{12} - Ex_7) \quad (19)$$

$$\eta_{ex,rec} = \frac{(Ex_{rec} + Ex_2 + Ex_{12} - Ex_{dest,rec})}{(Ex_{rec} + Ex_2 + Ex_{12})} \times 100 \quad (20)$$

Similarly, exergy destroyed and the exergetic efficiency can be calculated for the other components.

## 4. Results and Discussions

This section describes first the base case performance of the combined cycle at first stage pressure ratio 3 and second stage pressure ratio 1.5. Then the parametric analyses on energetic as well as exergetic performance have been discussed for the combined cycle. Code has been developed on C language for the thermodynamic analysis and properties of carbon dioxide have been obtained utilizing the RefpropMini software.

### 4.1 Base Case Performance

The base case performance of the combined cycle is shown in Table 2.

*Table 2.Base case performance data.*

| Characteristics | Value |
| --- | --- |
| Compressor pressure ratio (First stage) | 3 |
| Compressor pressure ratio (Second stage) | 1.5 |
| Gas turbine inlet temperature | 900 $^O$C |
| Total solar insolation on dish | 1411 kW |
| Net GT power | 243.54 kW |
| HRSG Steam generation rate | 698.9 kg/hr. |
| Net steam turbine power | 200.1 kW |
| Net total power | 443.64 kW |
| Overall thermal efficiency | 31.44% |

## 4.2 Parametric Study

This sub-section shows the parametric study of the combined cycle. The parametric study has been considered for the following cases:

a) Thermodynamic energetic performance has been evaluated for varying second stage pressure ratio and fixed first stage pressure ratio of 3 of the compressor and fixed gas turbine inlet temperature of $900^O$C.

b) Thermodynamic performance has been evaluated for the varying second stage pressure ratio as well as varying gas turbine inlet temperature. The gas turbine inlet temperature has been varied from $625^O$C to $900^O$C, which is possible to achieve with the type of receiver considered in the present study.

c) Exergetic performance has also been evaluated for the solar dish, receiver, GT II or power turbine, HRSG and stack. Parametric exergetic performance has also been evaluated for the varying second stage pressure ratio, fixed first stage pressure ratio of 3 of the compressor and fixed gas turbine inlet temperature of $900^O$C.

Figure 7 shows the net work, required solar energy and thermal efficiency of the GT cycle for the varying second stage pressure ratio and fixed first stage pressure ratio 3. The temperature of carbon dioxide increases with the increase of second stage pressure ratio.
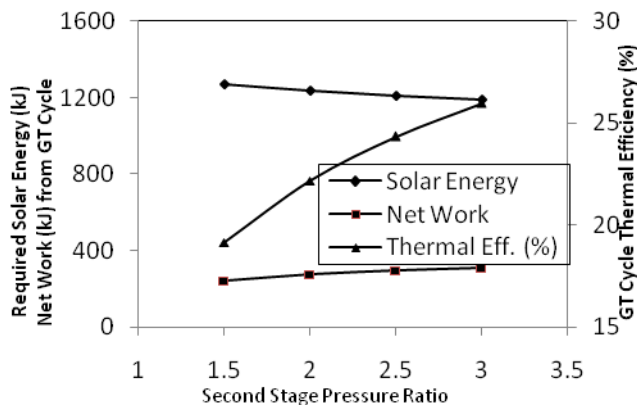


*Figure 7. Required solar energy, net work and thermal efficiency of GT block.*

Since the gas turbine inlet temperature (TIT) is fixed at $900^O$C and the temperature of carbon dioxide increases with the increase of second stage pressure ratio, the solar energy required to achieve the TIT decreases with the increase of pressure ratio. Since the net work obtained from the gas turbine cycle increases and the required solar energy decreases with the increase of second stage pressure ratio, the thermal efficiency increases with the increase of second stage pressure ratio.

With the increase of second stage pressure ratio, temperature of carbon dioxide is reducing at the end of second stage expansion, which results the decrease of mass flow rate of steam generation in HRSG. Hence, the net work obtained from the steam turbine is also getting reduced with the increase of second stage pressure ratio as shown in Figure 8.

Figure 9 shows the net work obtained from gas turbine cycle for varying gas turbine inlet temperature and varying second stage pressure ratio, which has been varied from 1.5 to 3 and at the interval of 0.5. It has been observed that net work obtained from GT cycle increases when second stage pressure ratio increases. For a fixed TIT, net work obtained

is higher at higher second stage pressure ratio since the enthalpy difference between entry and exit of second stage gas turbine is higher.

The variation of GT cycle thermal efficiency at varying gas turbine inlet temperature and second stage pressure ratio is shown in Figure 10. The thermal efficiency increases with the increase of second stage pressure ratio. This is due to the fact that solar thermal energy required to heat $CO_2$ to the gas turbine inlet temperature decreases with the increase of pressure ratio and also the net work obtained increases with the increase of pressure ratio.
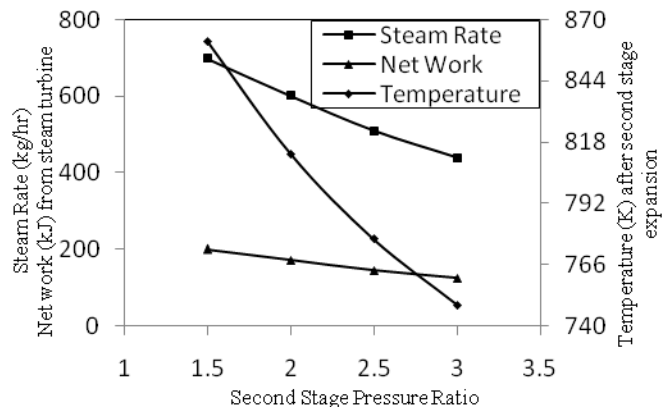


*Figure 8. Temperature after second stage expansion, steam rate and net work from HRSG cycle.*
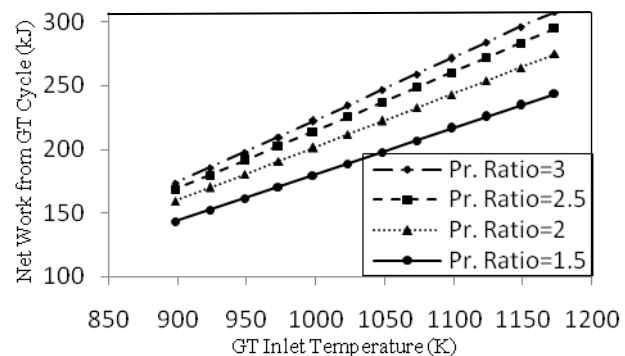


*Figure 9. Net work from GT cycle for varyingTIT and second stage pressure ratio.*
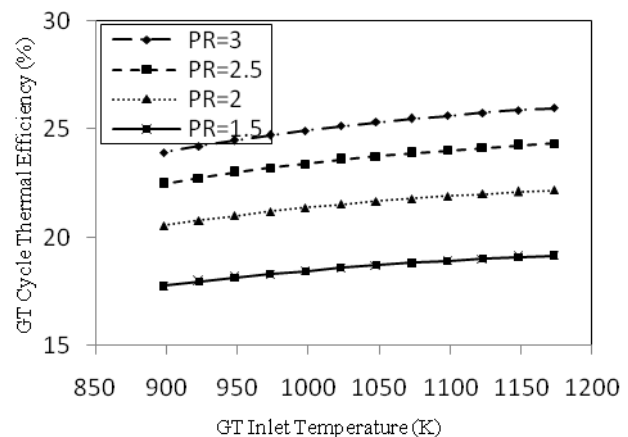


*Figure 10. GT cycle thermal efficiency for varyingTIT and varying second stage pressure ratio.*

Figure 11 shows the variation of steam turbine work with varying second stage pressure ratio and gas turbine inlet temperature. It is evident from the figure that steam turbine work is higher for lower second stage pressure ratio. This is due to the fact that steam rate is lower for the higher second stage pressure ratio, as shown in Figure 12, since the temperature of carbon dioxide after second stage expansion is lower at higher second stage pressure ratio, as shown in Figure 13.
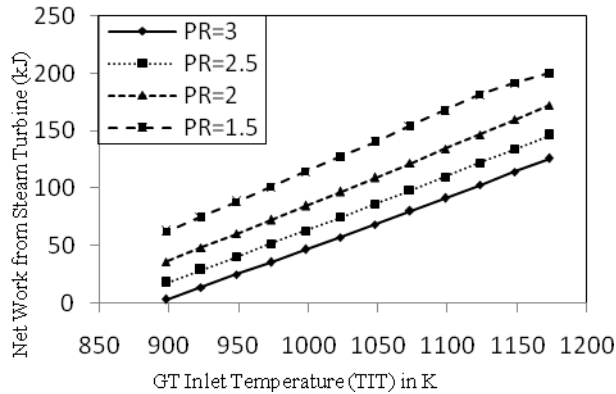


*Figure 11. Net work from steam turbine for varying TIT and varying second stage pressure ratio.*
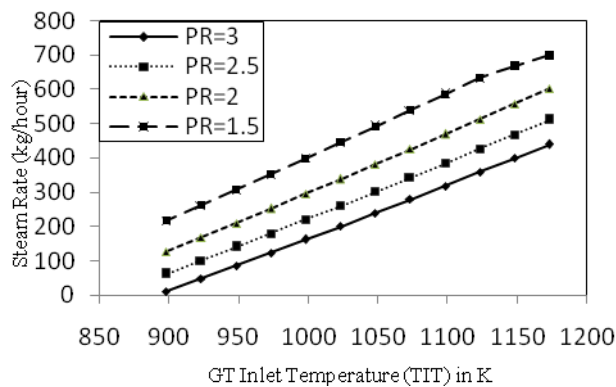


*Figure 12.Steam rate for varying TIT and varying second stage pressure ratio.*
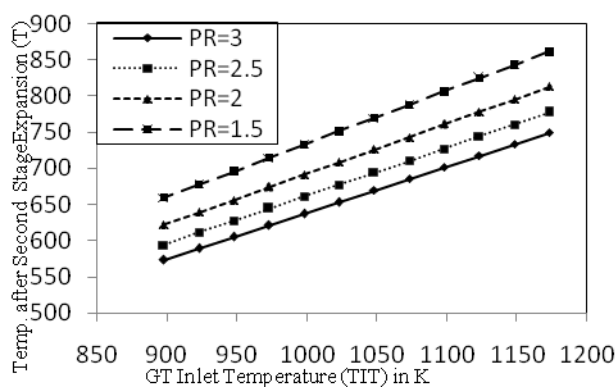


*Figure 13.Variation of temp.after second stage expansion with varying TIT and varying second stage pressure ratio.*

The variation of net work from GT, ST and total work output from combined cycle is shown in Figure 14 at fixed gas turbine inlet temperature of $900^O$ C. The net work output from GT block increases but steam turbine work decreases with the increase of second stage pressure ratio as explained earlier. Their combined effect on total work output is that it initially increases, reaches the maximum

value at pressure ratio 2 and then decreases with the increase of second stage pressure ratio.

Figure 15 shows that the work obtained from GT, ST increases with the increase of gas turbine inlet temperature. The overall thermal efficiency also takes an upward trend with the increase of gas turbine inlet temperature.
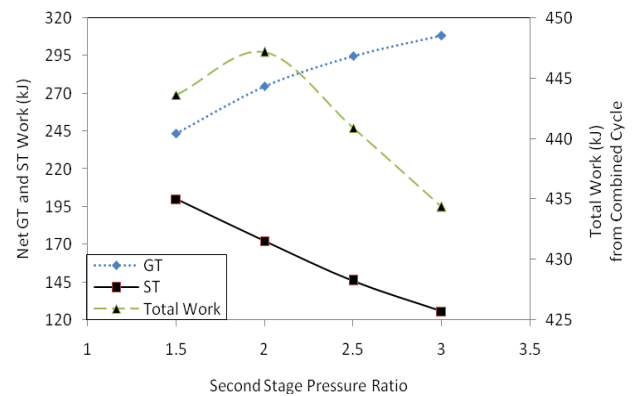


*Figure 14. Variation of GT work, ST work and total work varying second stage pressure ratio.*
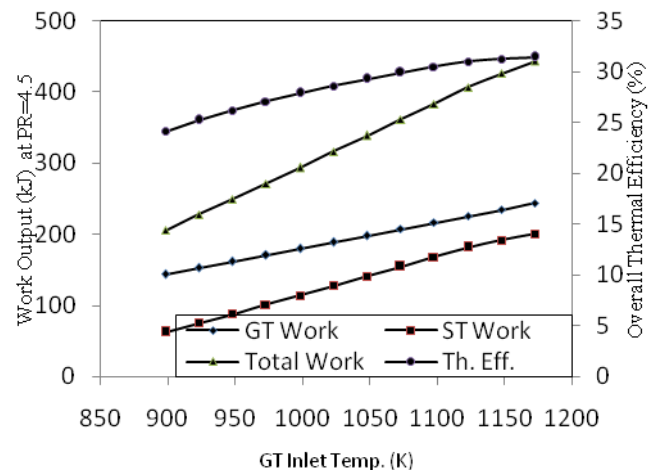


*Figure 15. Variation of GT work, ST work, total work and overall thermal efficiency at first stage PR=3and second stage PR=1.5 with varying TIT.*

### 4.2.1 Parametric Analysis on Exergetic Performance

Figure 16 shows the lost exergy for different components (solar dish, solar receiver, power turbine, HRSG) and also the stack loss for the conceptualized combined cycle plant at pressure ratio of 4.5. It is evident that exergy destruction is highest for solar receiver. The exergy loss in case of solar receiver is the highest because heat is transferred from a very hightemperature of heat source to a comparatively low temperature solar receiver. Considerable amount of exergy is also destroyed at stack and solar dish. That's why parametric analyses of these components have been discussed subsequently.

The effect of varying pressure ratios on exergy destroyed and the exergetic efficiency of solar receiver is shown in Figure 17. The decrease of exergy destruction with increased pressure ratio is due to the fact that steam rate is reducing with the increase of second stage pressure ratioand hence amount of heat energy required to superheat the steam in solar receiver is also reducing, resulting in decrease in associated exergy. Since the exergy destruction is reducing with the increase of pressure ratio, exergetic efficiency of the solar receiver is increasing with the increase of second stage pressure ratio.
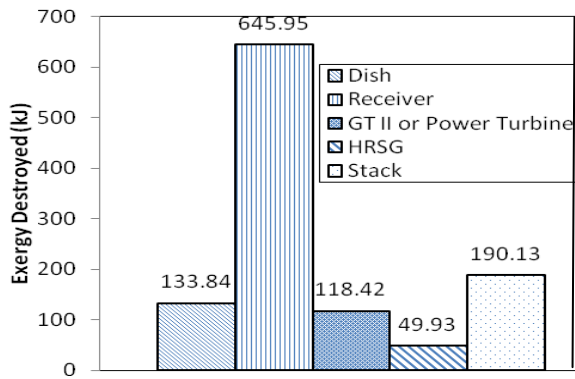
*Figure 16. Exergy destruction for different components at PR=4.5.*
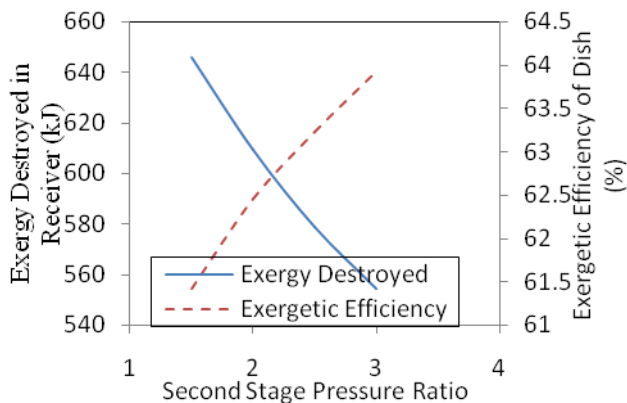


*Figure 17: Variation of exergy destroyed and exergetic efficiency of solar receiver with second stage pressure ratio.*

For the dish sub-system, the exergetic performance is improving i.e. the exergy destruction is reducing with the increase of second stage pressure ratio. This is due to the fact that with the increase of pressure ratio of the second stage compressor, the amount of heat energy required in the solar receiver is reducing due to reduced steam rate, resulting in reduction in associated exergy. But the exergetic efficiency curve assumes a straight line at 90% since the dish efficiency has been considered as 0.9. The variation of exergy destroyed and the exergetic efficiency of dish sub-system is shown in Figure 18.
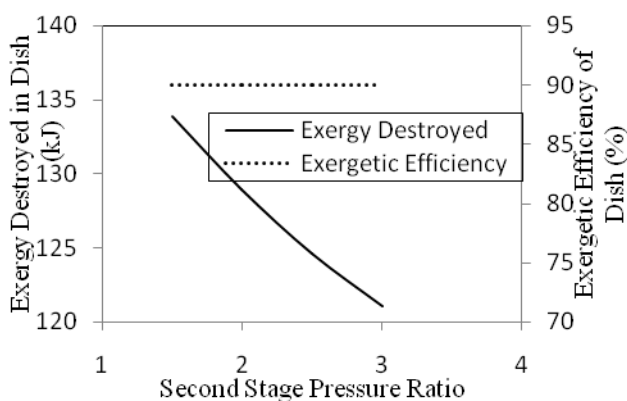


*Figure 18. Variation of exergy destroyed and exergetic efficiency of dish sub-system with second stage pressure ratio.*
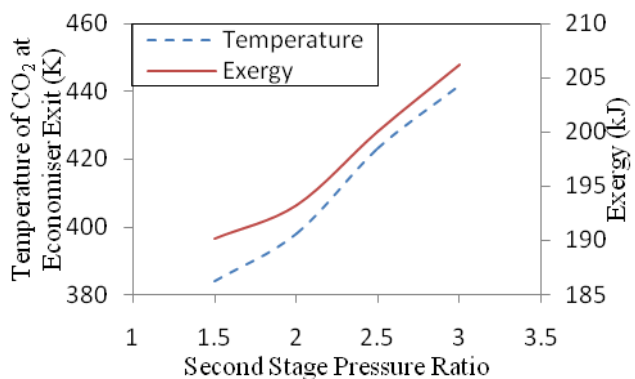


*Figure 19: Stack exergy variation with varying second stage pressure ratio.*

Figure 19 shows the variation of stack temperature and stack exergy with varying second stage pressure ratio. Due to the combined effect of minimum pinch point temperature difference of 15 $^O$C and reduced mass flow rate of steam with increasing second stage pressure ratio, the temperature of carbon dioxide at the economizer exit is increasing with the increase of second stage pressure ratio. Since the temperature is increasing, associated exergy is also increasing with the increase of second stage pressure ratio.

**5. Conclusions**

The present study proposes a conceptual configuration of solar dish based combined cycle plant: topping GT cycle with carbon dioxide as the working fluid and a bottoming HRSG plant.

• Carbon dioxide is a promising option for the topping gas turbine plant since the carbon dioxide is denser than air and hence, the size of the components like compressor, gas turbine etc. will be smaller in comparison to air.

• Parametric Analysis of the combined cycle with carbon dioxideas the working fluid for the topping Brayton cycle, has been done for the varying second stage pressure ratio and for the varying gas turbine inlet temperature but at fixed first stage pressure ratio of 3. It suggests that work output from combined cycle increases initially, reaches a maximum value at second stage pressure ratio of 2 and then decreases. The total work output is maximum at second stage pressure ratio of 2.

• For a fixed second stage pressure ratio, the total work output also increases with the increase of gas turbine inlet temperature and it is maximum at gas turbine inlet temperature of $900^O$ C. So, the combined cycle should be operated at second stage pressure ratio of 2 and TIT $900^O$ C.The overall thermal efficiency at this condition is 32.9%.

• From the exergetic analysis, it is observed that at the exit of economiser, the carbon dioxide is having sufficient exergy, which can be utilized further. If the combined cycle plant is operated at second stage pressure ratio of 2 and TIT $900^O$ C, the temperature of carbon dioxide at the exit of economiser is $125^O$ C. This heat can be utilized in other applications like ethanol distillation, process heat applications etc.

• Although the combined cycle option is more expensive in terms of initial investment than a single Brayton cycle, it might be noted that for a concentrating solar power (CSP) plant, the solar concentrator-receiver system takes the largest share of space and cost. Adding a bottoming cycle would add both to the power output and the overall efficiency without adding significant additional

cost and space. As the present study revealed, incorporation of a simple HRSG downstream of gas turbine increased the power output of the plant from 243.54kW to 443.64kW in the base case. The thermal efficiency also increased by about 10%

## Nomenclature

| | |
|---|---|
| G | Generator |
| $h$ | Enthalpy |
| $p$ | Absolute pressure (bar) |
| $T$ | Absolute temperature (K) |
| $\eta_C$ | Isentropic efficiency of compression |
| $\eta_E$ | Isentropic efficiency of expansion |
| $m$ | Mass flow rate of gas (kg/s) |
| $W_{net,GT}$ | Net work from GT cycle (kJ) |
| $Q$ | Heat energy (kJ) |
| $\eta_{dish}$ | Dish efficiency |
| $\eta_{receiver}$ | Receiver efficiency |
| $\eta_{GT}$ | Isentropic efficiency of gas turbine |
| $\eta_G$ | Generator efficiency |
| $\eta_{th}$ | Thermal efficiency |
| $\eta_{ST}$ | Isentropic efficiency of steam turbine |
| $m_w$ | Mass flow rate of water (kg/s) |
| $W_{ST}$ | Steam turbine work (kJ) |
| TIT | Gas turbine inlet temperature (K) |
| GT | Gas turbine |
| PR | Pressure ratio |
| $Ex$ | Exergy |

### Subscript

| | |
|---|---|
| $dest$ | Destroyed |
| $rec$ | Receiver |

## References

[1] German Aerospace Center, DLR, Final Report on Concentrating Solar Power for the Mediterranean Region, German Aerospace Center (DLR), Institute of Technical Thermodynamics, 2005.

[2] Sukhatme, S. P., *Solar Energy Principles of Thermal Collection and Storage,* 2nd Ed. New Delhi: Tata McGraw-Hill Publishing Company Limited, 2008.

[3] CSP Alliance The Economic and Reliability Benefits of CSP with Thermal Energy Storage: Recent Studies and Research Needs (Accessed 2013): :http://www.brightsourceenergy.com/stuff/contentmgr/files/0/e21370463a103edc99138a90deb172d5/attachment/cspa_report_dec_2012_ver1.0.pdf.

[4] Li, Lifang, Dubowsky, Steven, A new design approach for solar concentrating parabolic dish based on optimized flexiblepetals, *Mechanism and Machine Theory*, 46, 1536-1548, 2011.

[5] Wu, Shuang-Ying, Xiao, Lan, Cao, Yiding., *et al.*, Convection heat loss from cavity receiver in parabolic dish solar thermal power system: A review, *Solar Energy,* 84, 1342-1355, 2010.

[6] Kribus, A., Zaibel, R., Carey, D., *et al.*, A Solar-Driven Combined Cycle Power Plant, *Solar Energy*, 62 121-129, 1998.

[7] Buck, Reiner., Barth, Christian., Eck, Markus., *et al.*, Dual-receiver concept for solar towers, *Solar Energy*, 80, 1249-1254, 2006.

[8] Agrawal, N., Bhattacharyya, S., Studies on a two-stage transcritical carbon dioxideheat pump cycle with flash intercooling, *Applied Thermal Engineering,* 27, 299-305, 2007.

[9] Xu, Chao, Wang, Zhifeng., Li, Xin., *et al.*, Energy and exergy analysis of solar power tower plants, *Applied Thermal Engineering*, 31, 3904-3913, 2011.

[10] Chacartegui, R., Escalona, J.M. Munoz de., et al., Alternative cycles based on carbon dioxide for central receiver solar power plants, *Applied Thermal Engineering,* 31, 872-879, 2011.

[11] Kribus, A., Doron, P., Rubin, R., Karni, J., *et al.*, A Multistage Solar Receiver: The Route To High Temperature, *Solar Energy*, 67, 3–11, 1999.

[12] Mukhopadhyay, S., Ghosh, S., Energetic And Exergetic Performance Evaluation of A Solar Dish Based Dual Receiver Combined Cycle, *International Journal of Emerging Technology and Advanced Engineering,* 3, 234-243, 2013.

[13] Heller, P., Pfander, M., Denk, T., *et al.*, Test And Evaluation of A Solar Powered Gas Turbine System, *Solar Energy*, 80, 1225–1230, 2006.

[14] Kehlhofer, R., Hannemann, F., Stirnimann, F., *et al., Combined Cycle Gas & Steam Turbine Power Plant*s, 3rd Ed., Oklahoma: PennWell Corporation, 2009.

[15] Abbas, M., Boumeddane, B., Said, N., *et al.,* Dish Stirling technology: A 100 MW solar power plant using hydrogen for Algeria, *International Journal of Hydrogen Energy*, 36, 4305-4314, 2011.

[16] Ghosh, S., De, S., Thermodynamic Performance Simulation Of A Coal Gasification And SOFC Based Combined Cogeneration Plant By Energy And Exergy Analysis, *Int. J. Exergy*, 2(4), 366-384, 2005.